Light Vector Meson Production at HERA

Alexander Proskuryakov for the H1 and ZEUS collaborations

Moscow State University, 119899 Moscow, Russia

Abstract. Recent results from HERA on exclusive vector meson production are reviewed. The diffractive reaction $\gamma^\star p \to Vp$ ($V = \rho^0, \omega.\phi$) has been measured at photon-proton centre-of-mass energies $20 < W < 160$ GeV, for photon virtualities $Q^2 < 60$ GeV^2 and for $|t|$ up to 11 GeV^2, where t is the square of the four-momentum transferred at the proton vertex. The $\gamma^\star p \to Vp$ cross section as a function of W, Q^2 and t is presented. The polarisation properties of the ρ^0 produced at low and high Q^2 are discussed. The data are compared with perturbative QCD calculations.

1 Introduction

A detailed description of results on the diffractive production of the vector mesons by real and virtual photons is available in [1,2].

1.1 Kinematics

Figure 1 shows a schematic diagram for exclusive vector meson production in the reaction $ep \to epV$, where V stands for a vector meson (ρ^0, ω, ϕ, J/ψ...).

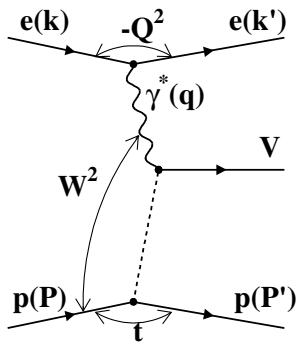

Fig. 1. Schematic diagram for exclusive vector meson production

The kinematics of this reaction is described by the following variables:

- the negative of the four-momentum squared of the exchanged photon, $Q^2 = -(k-k')^2$, where $k(k')$ is the four-momentum of the incident (scattered) electron;
- the centre-of-mass energy of the photon-proton system, $W = \sqrt{(q+P)^2}$, where q and P are the four-momenta of the exchanged photon and the incident proton respectively;
- the Bjorken variable $y = pq/pk$;
- the four-momentum transfer squared at the proton vertex, $t = (P-P')^2$, where P' is the four-momentum of the scattered proton;
- the angle between the vector meson production plane and the electron scattering plane, Φ.

The kinematics of the vector meson decay (in the following only two particle decay is considered) is described by the polar angle θ and the azimuthal angle ϕ in the s-channel helicity frame [3], in which the quantisation axis is defined as the direction of the momentum of the final-state proton in the V rest frame.

1.2 Cross section

The cross section of exclusive vector meson production from virtual photons has contributions from longitudinal (helicity 0 state) and transverse (helicity ± 1 state) photons. The differential electron-proton cross section is related to the virtual longitudinal and transverse photon-proton cross sections $\sigma_L^{\gamma^\star p}$ and $\sigma_T^{\gamma^\star p}$ as:

$$\frac{d\sigma^{ep}}{dydQ^2} = \Gamma_T(y,Q^2)(\sigma_T^{\gamma^\star p} + \epsilon\sigma_L^{\gamma^\star p}), \tag{1}$$

with the flux of transverse photons given by

$$\Gamma_T = \frac{\alpha_{em}}{2\pi}\frac{1+(1-y)^2-2(1-y)Q^2_{min}/Q^2}{yQ^2}, \tag{2}$$

and the polarisation parameter ϵ defined as

$$\epsilon = \frac{2(1-y)}{1+(1-y)^2-2(1-y)Q^2_{min}/Q^2}, \tag{3}$$

where $Q^2_{min} \simeq m_e^2 y^2/(1-y)$ is the minimum kinematically allowed value of Q^2. In the kinematic region covered by the HERA data the value of the polarisation parameter ϵ is close to unity. The virtual photon-proton cross section, $\sigma^{\gamma^\star p} = \sigma_T^{\gamma^\star p} + \epsilon\sigma_L^{\gamma^\star p}$, can be related to the total cross section, $\sigma_{TOT}^{\gamma^\star p} = \sigma_T^{\gamma^\star p} + \sigma_L^{\gamma^\star p}$, through the relation:

$$\sigma_{TOT}^{\gamma^\star p} = \frac{1+R}{1+\epsilon R}\sigma^{\gamma^\star p}, \tag{4}$$

where $R = \sigma_L^{\gamma^\star p}/\sigma_T^{\gamma^\star p}$ is the ratio of the longitudinal and the transverse cross sections.

1.3 Decay angular distributions

The decay angular distributions for the reaction $ep \to e\rho^0 p$ can be written as [3]:

$$
\begin{aligned}
W(\cos\theta,\phi,\Phi) = \frac{3}{4\pi}\Bigg[&\frac{1}{2}(1-r^{04}_{00}) + \frac{1}{2}(3r^{04}_{00}-1)\cos^2\theta \\
&-\sqrt{2}\mathrm{Re}\{r^{04}_{10}\}\sin 2\theta\cos\phi - r^{04}_{1-1}\sin^2\theta\cos 2\phi \\
&-\epsilon\cos 2\Phi(r^{1}_{11}\sin^2\theta + r^{1}_{00}\cos^2\theta - \sqrt{2}\mathrm{Re}\{r^{1}_{10}\}\sin 2\theta\cos\phi - r^{1}_{1-1}\sin^2\theta\cos 2\phi) \\
&-\epsilon\sin 2\Phi(\sqrt{2}\mathrm{Im}\{r^{2}_{10}\}\sin 2\theta\sin\phi + \mathrm{Im}\{r^{2}_{1-1}\}\sin^2\theta\sin 2\phi) \\
&+\sqrt{2\epsilon(1+\epsilon)}\cos\Phi(r^{5}_{11}\sin^2\theta + r^{5}_{00}\cos^2\theta \\
&-\sqrt{2}\mathrm{Re}\{r^{5}_{10}\}\sin 2\theta\cos\phi - r^{5}_{1-1}\sin^2\theta\cos 2\phi) \\
&+\sqrt{2\epsilon(1+\epsilon)}\sin\Phi(\sqrt{2}\mathrm{Im}\{r^{6}_{10}\}\sin 2\theta\sin\phi + \mathrm{Im}\{r^{6}_{1-1}\}\sin^2\theta\sin 2\phi)\Bigg]. \qquad (5)
\end{aligned}
$$

The spin-density matrix elements r^{04}_{ij}, r^{α}_{ij} are the combinations of the helicity amplitudes $T_{\lambda_V\lambda_\gamma}$ (the nucleons helicities are omitted), where λ_V and λ_γ are the helicities of the vector meson and the photon respectively.

The assumption of helicity conservation in the photon-proton centre-of-mass frame (SCHC) reads:

$$T_{\lambda_V\lambda_\gamma} = T_{\lambda_V\lambda_\gamma}\delta_{\lambda_V\lambda_\gamma}. \qquad (6)$$

Under this assumption all matrix elements except r^{04}_{00}, r^{1}_{1-1}, $\mathrm{Im}\{r^{2}_{1-1}\}$, $\mathrm{Re}\{r^{5}_{10}\}$ and $\mathrm{Im}\{r^{6}_{10}\}$ are zero. The remaining matrix elements are related via:

$$r^{1}_{1-1} + \mathrm{Im}\{r^{2}_{1-1}\} = 0, \qquad (7)$$

$$\mathrm{Re}\{r^{5}_{10}\} + \mathrm{Im}\{r^{6}_{10}\} = 0. \qquad (8)$$

The angular distribution in the case of SCHC depends on two angles, θ and $\psi = \phi - \Phi$:

$$
\begin{aligned}
W(\cos\theta,\psi) = \frac{3}{4\pi}\Bigg[&\frac{1}{2}(1-r^{04}_{00}) + \frac{1}{2}(3r^{04}_{00}-1)\cos^2\theta \\
&+\epsilon r^{1}_{1-1}\sin^2\theta\cos 2\psi - 2\sqrt{2\epsilon(1+\epsilon)}\mathrm{Re}\{r^{5}_{10}\}\sin 2\theta\cos\psi\Bigg]. \qquad (9)
\end{aligned}
$$

The SCHC hypothesis allows the direct determination of the ratio $R = \sigma^{\gamma^\star p}_L/\sigma^{\gamma^\star p}_T$ from the value of r^{04}_{00}:

$$R = \frac{r^{04}_{00}}{\epsilon(1-r^{04}_{00})}. \qquad (10)$$

1.4 Theoretical models

Exclusive production of light vector mesons has been studied in a wide range of W and Q^2 in fixed target experiments [1,4] and at HERA [5,6]. For $W >$

10 GeV and at low photon virtuality these reactions have the characteristics of a soft diffractive process: a cross section rising weakly with the centre-of-mass energy, a sharp forward diffractive peak in the differential t distribution and s-channel helicity conservation (SCHC). These features are well described within the framework of Regge phenomenology [7] and the Vector Dominance Model (VDM) [8,9]. In this approach the energy dependence of exclusive vector meson production at high energies is determined by the exchange of a Pomeron trajectory:

$$\frac{d\sigma}{d|t|} \propto e^{-b_0|t|}\left(\frac{W^2}{W_0^2}\right)^{2(\alpha(t)-1)}, \tag{11}$$

where the Pomeron trajectory is parameterised as $\alpha(t) = \alpha(0) + \alpha' t = 1.08 + 0.25t$ [10]. The W dependence of cross section in the HERA kinematic region can approximately be parameterised by a simple power behaviour, W^δ, where $\delta \simeq 4(\alpha(0) - \alpha'/b - 1)$. The slope of the differential t distribution depends on the energy as $b = b_0 + 2\alpha' ln(W^2/W_0^2)$.

The same approach fails to describe the energy dependence of the cross section for elastic J/ψ photoproduction measured at HERA [11]. The rapid rise with energy of the elastic J/ψ photoproduction cross section is consistent with a perturbative QCD calculation [12]. The hard scale for this reaction is given by the charm quark mass.

The hard scale can also be provided by the photon virtuality Q^2. Exclusive electroproduction at high values of Q^2 has been the subject of many theoretical investigations (see e.g. [13–18]). The main prediction of the perturbative QCD models is a fast increase of the cross section with W, connected with the Q^2 evolution of the gluon density of the proton $xg(x, Q^2)$. The Q^2 dependence for the longitudinal vector meson production, which dominates at high Q^2, is $\sigma_L^{\gamma^\star p} \sim (xg(x, Q^2))^2/Q^6$. The QCD models predict also universal, flavor and energy independent, t dependence for this exclusive diffractive process.

Recent calculations of the helicity amplitudes for the reaction $\gamma^\star p \to \rho^0 p$, performed in the framework of perturbative QCD [19–21] predict small violations of SCHC. The largest helicity non-conserving amplitude is expected to be T_{01}, which describes the production of longitudinally polarised vector mesons from transverse photons.

2 Results

2.1 The W dependence of the $\gamma^\star p \to Vp$ cross sections

Figure 2 shows the energy dependence of elastic ρ^0, ω, ϕ and J/ψ photoproduction ($Q^2 \simeq 0$ GeV^2) cross sections measured at HERA and fixed target experiments. The W dependence of the cross section for light vector meson photoproduction is well parameterised at high energy as $\sigma^{\gamma p} \propto W^\delta$ with $\delta \simeq 0.22$. This weak energy dependence is in agreement with the 'soft' Pomeron parameterisation of eq. (11).

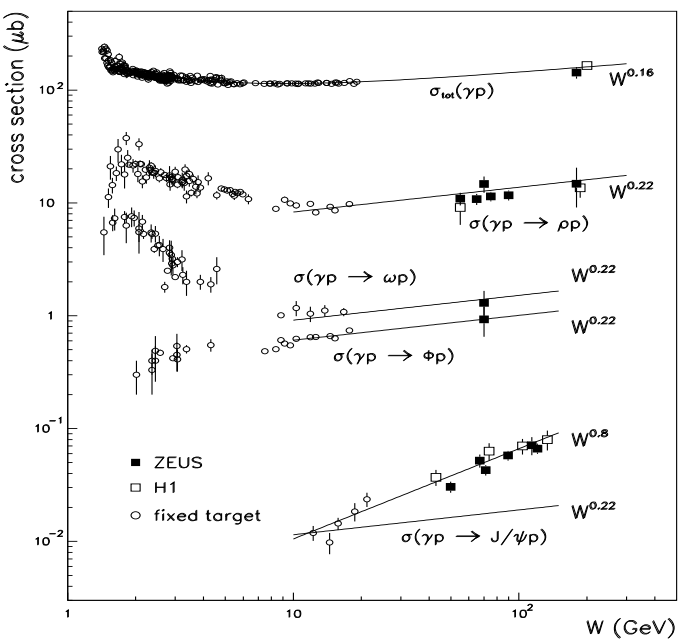

Fig. 2. The energy dependence of the total photoproduction and vector meson photoproduction cross sections for fixed target and HERA experiments.

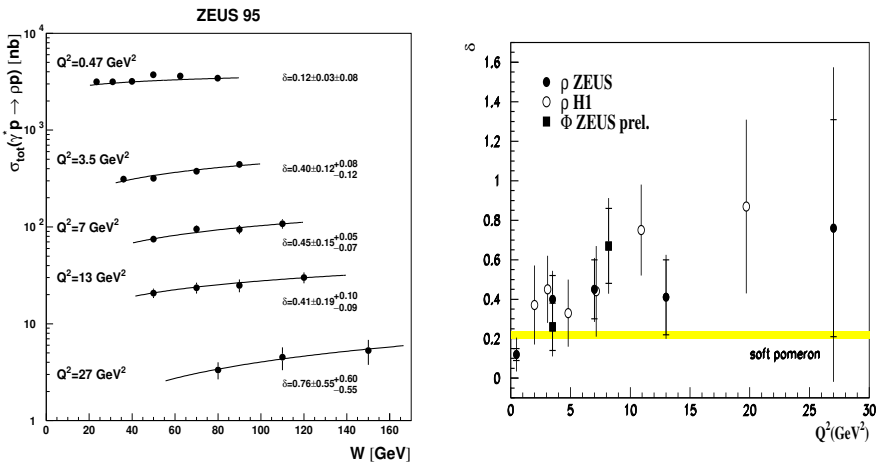

Fig. 3. The energy dependence of exclusive ρ^0 production cross sections for different values of Q^2. The lines represent the function $\sigma \propto W^{\delta}$ fitted to the data.

Fig. 4. The values of δ as a function of Q^2 for exclusive production of ρ^0 and ϕ mesons.

In contrast, the rapid rise with energy of the elastic J/ψ photoproduction cross section is consistent with a perturbative QCD calculation [12].

The W dependence of the exclusive ρ^0 production cross section at different values of Q^2 is shown in Fig. 3. The lines represent the result of a fit to the data with a function of type $\sigma \propto W^{\delta}$. The results of the fit are summarised in Fig. 4. As can be seen from Fig. 4, the W dependence of the cross section for the reaction $\gamma^{\star}p \to Vp$ is consistent with the 'soft' Pomeron approach at low values of Q^2. In the region of high Q^2, where QCD based models predict a steeper cross section dependence on W, there is an indication that the rise of the cross section becomes faster.

2.2 The Q^2 dependence of the $\gamma^{\star}p \to Vp$ cross sections

The cross section for exclusive ρ^0 production as a function of Q^2 is shown in Fig. 5. The Q^2 dependence of the $\gamma^{\star}p \to \rho^0 p$ cross section is well described in a wide range of Q^2 by the function $d\sigma/dQ^2 \propto 1/(1+Q^2/M_{\rho}^2)^n$, with $n = 2.28 \pm 0.06$. The curves shown in Fig. 5 represent the predictions of QCD [17,18] and Generalized VDM [9].

Figure 6 shows the ratio of the ϕ and ω production cross sections to that for the ρ^0 meson as a function of Q^2. The ratios in the high Q^2 region are consistent with the prediction of QCD models.

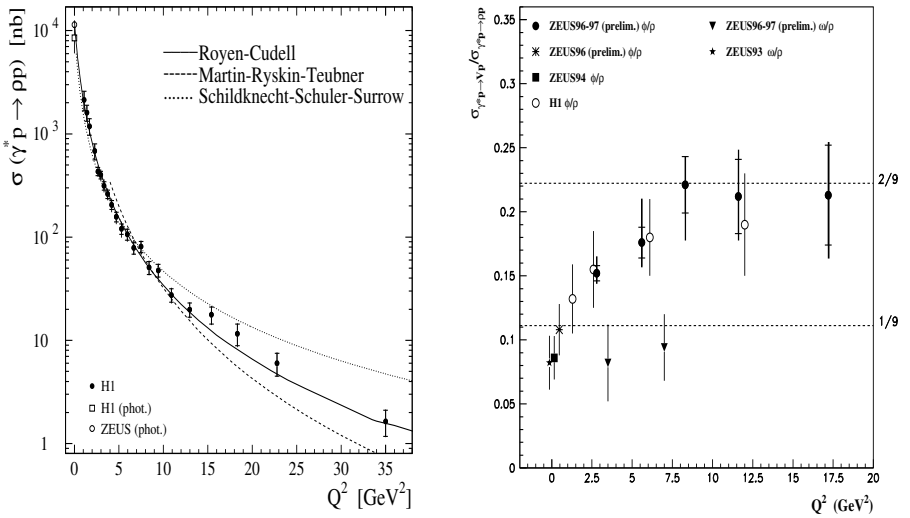

Fig. 5. The Q^2 dependence of the exclusive ρ^0 production cross section. The curves represent the predictions of the QCD models [17,18] and Generalized VDM [9].

Fig. 6. Ratios of ϕ and ω cross sections to that for the ρ^0 meson as a functions of Q^2.

2.3 The t dependence of the $\gamma^\star p \to Vp$ cross sections

The exponential t dependence of the $\gamma^\star p \to Vp$ cross section is a typical characteristic of diffractive processes. The slope parameter b, which is related in optical models to the sizes of the interacting particles, is expected to depend on the photon virtuality. Figure 7 shows the slope parameter for exclusive ρ production as a function of Q^2. Despite large statistical errors of the experimental data these results indicate that the slope b decreases with Q^2, approaching the value of $b \simeq 4 - 5$ GeV^{-2}.

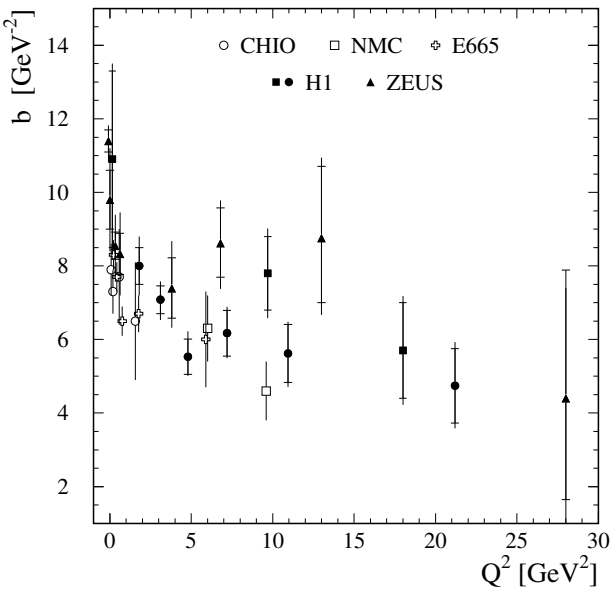

Fig. 7. The slope parameter b as a function of Q^2 for exclusive ρ^0 production.

The slope parameter also depends on the vector meson mass. The value of b is [5,11] $9.8 \pm 0.8(\text{stat}) \pm 1.1(\text{syst})$ GeV^{-2}, $7.3 \pm 1.0(\text{stat}) \pm 0.8(\text{syst})$ GeV^{-2} and $4.0 \pm 0.4(\text{stat})^{+0.6}_{-0.7}(\text{syst})$ GeV^{-2}, for photoproduction of ρ^0, ϕ and J/ψ mesons respectively.

The differential t distribution at low $|t|$ is well described by Regge phenomenology assuming that the exchange of the Pomeron trajectory dominates at high enough energies. The parameters of the Pomeron trajectory can be measured by studying the energy dependence of $d\sigma/dt$ at different t values (see eq. 11). Figure 8 shows the W dependence for the elastic ρ^0 photoproduction cross section at fixed t values. The resulting Pomeron trajectory, shown in Fig. 9, is $\alpha(t) = (1.096 \pm 0.021) + (0.125 \pm 0.038)t$.

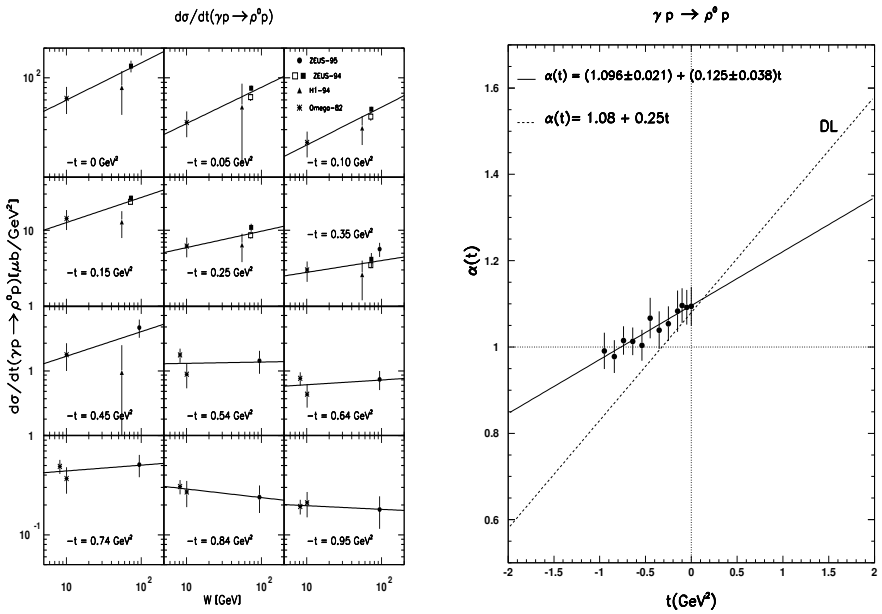

Fig. 8. Cross section for elastic ρ^0 photoproduction as a function of W at different values of t. The W dependence is fitted by $d\sigma/dt \propto (W^2)^{2\alpha(t)-2}$.

Fig. 9. The Pomeron trajectory determined from the reaction $\gamma p \to \rho^0 p$. The dots are the values of the trajectory at a given t as determined from figure 8. The full line is the result of a linear fit to these values. The Pomeron trajectory given in [10] is shown as the dashed line.

2.4 Decay angular distributions

The analysis of vector meson decay distribution provides important information about helicity properties of the reaction $\gamma^\star p \to Vp$. In the case of unpolarised beams, the angular distributions are determined by 15 spin density matrix elements (see eq. 5), which are the combinations of the helicity amplitudes $T_{\lambda_V,\lambda_\gamma}$. The full set of spin density matrix elements has been measured for exclusive ρ^0 production. The most significant deviation from the expectation of SCHC is observed for the matrix element r^5_{00}. This matrix element is proportional to the interference between the helicity non-flip amplitude T_{00} and the helicity single-flip amplitude T_{01}. The size of this effect can be quantified by the ratio of the helicity single-flip amplitude to the helicity conserving amplitudes $|T_{01}|/\sqrt{|T_{00}|^2 + |T_{11}|^2}$, which gives $(8 \pm 3)\%$ [6].

Figure 10 shows the 15 spin density matrix elements as a function of Q^2. The results of the QCD based calculations [20,21] shown in Fig. 10 are in good agreement with the data.

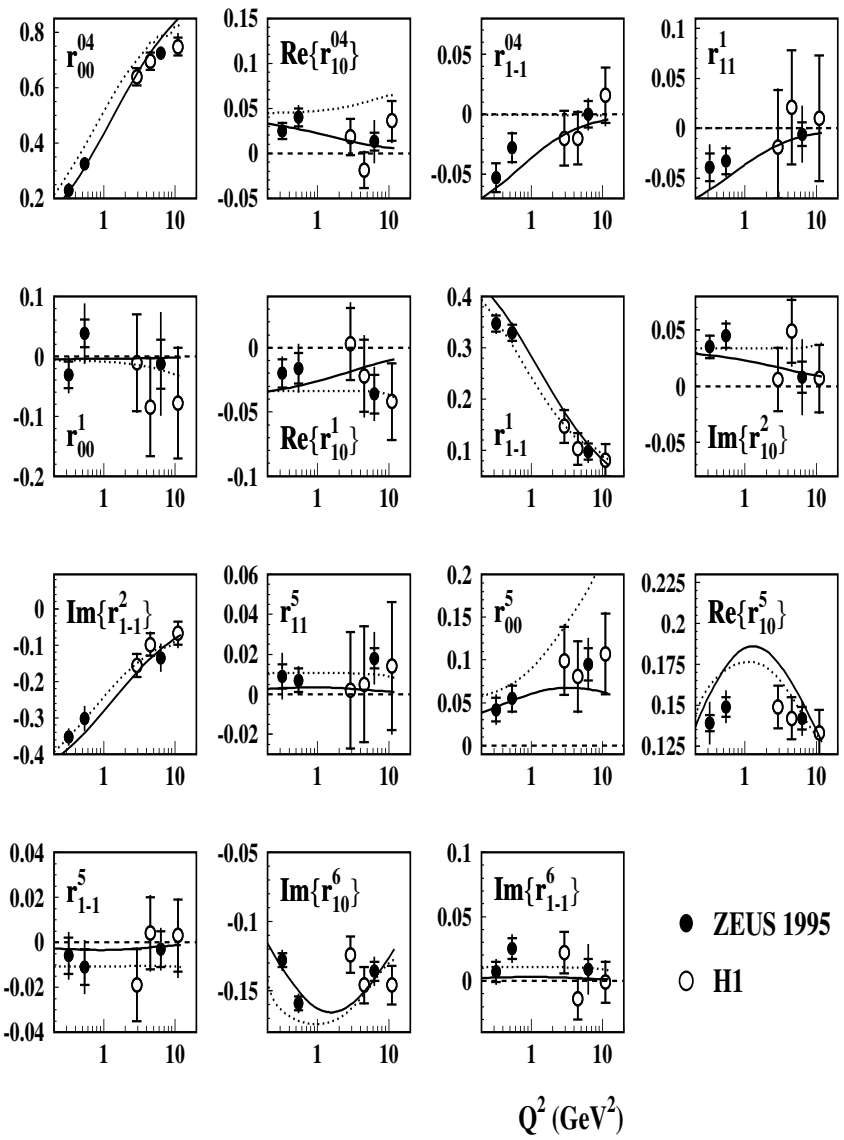

Fig. 10. The 15 spin density matrix elements as a function of Q^2. The full curves are the prediction of Ref. [20], the dotted curves the prediction of Ref. [21]. The dashed lines indicate the expectation of SCHC.

The ratio $R = \sigma_L^{\gamma^\star p}/\sigma_T^{\gamma^\star p}$, calculated according to eq. 10 (neglecting small violation of SCHC) , is displayed in Fig. 11 as a function of Q^2 for exclusive ρ^0 production. The curves represent the predictions of the QCD [17,18] and Generalized VDM [9]. Fig. 11 shows that the longitudinal photon-proton cross section dominates at large Q^2 and that the non-linear rise of R can be reproduced by the theoretical models.

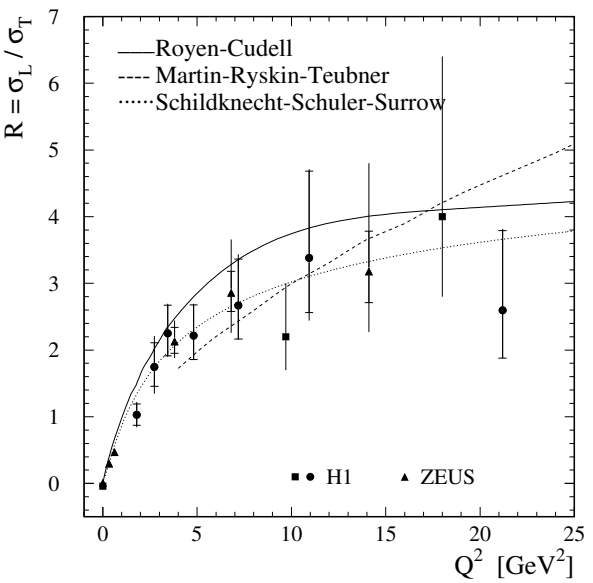

Fig. 11. The ratio of the longitudinal and transverse photon-proton cross sections as a function of Q^2. The curves represent the predictions of the QCD [17,18] and Generalized VDM [9].

3 Conclusions

- The energy dependence of the light vector meson production cross section exhibits a slow rise with W at low values of Q^2. There is an indication that in the region of high Q^2 this rise becomes faster, in agreement with predictions by QCD models. The cross section for exclusive J/ψ production shows a steep rise with W already a low photon virtualities.
- The Q^2 dependence of the $\gamma^\star p \to \rho^0 p$ cross section is well described (for $Q^2 > 1$ GeV^2) by the function $d\sigma/dQ^2 \propto 1/(1+Q^2/M_\rho)^n$, with $n = 2.24 \pm 0.09$. The ratios of the ϕ and ω production cross sections to that for the ρ^0 meson are consistent in the high Q^2 region with the predictions of QCD models.

- The t distribution for the exclusive vector meson production is well parameterised by an exponential dependence e^{bt}. The slope parameter b decreases with Q^2. The Pomeron trajectory, determined from the reaction of elastic ρ^0 photoproduction, is $\alpha(t) = (1.096 \pm 0.021) + (0.125 \pm 0.038)t$.
- The full set of spin density matrix elements measured for exclusive ρ^0 productions shows a small deviation from the SCHC hypothesis. The ratio of the longitudinal and transverse photon-proton cross sections exhibits a non-linear rise with Q^2. The theoretical models reproduce this behaviour.

References

1. T.H. Bauer et al., Rev. Mod. Phys. 50 (1978) 261.
2. J.A. Crittenden, Exclusive Production of Neutral Vector Mesons at the Electron-Proton Collider HERA, Springer Tracts in Modern Physics, Volume 140 (Springer, Berlin Heidelberg, 1997).
3. K. Schilling and G. Wolf, Nucl. Phys. B61 (1973) 381.
4. R.M. Egloff et al., Phys. Rev. Lett. 43 (1979) 657;
   R.M. Egloff et al., Phys. Rev. Lett. 43 (1979) 1545;
   J. Busenits et al., Phys. Rev. D40 (1989) 1;
   EMC Collab., J.J. Aubert et al., Phys. Lett. B161 (1985) 203;
   NMC Collab., M. Arneodo et al., Nucl. Phys. B429 (1994) 503;
   M.R. Adams et al., Z. Phys., C74 (1997) 237.
5. ZEUS Collab., M Derrick et al., Z. Phys. C69 (1995) 39;
   H1 Collab., S. Aid et al., Nucl. Phys. B463 (1996) 3;
   ZEUS Collab., M. Derrick et al., Phys. Lett. B377 (1996) 259;
   ZEUS Collab., M. Derrick et al., Z. Phys., C73 (1996) 73;
   ZEUS Collab., M. Derrick et al., Z. Phys. C73 (1997) 253;
   ZEUS Collab., J. Breitweg et al., Eur. Phys. J. C2 (1998) 247;
   ZEUS Collab., J. Breitweg et al., Eur. Phys. J. C6 (1999) 603.
6. H1 Collab., C. Adloff et al., DESY Report DESY 99-010, hep-ex/9902019 (1999);
   ZEUS Collab., J. Breitweg et al., DESY Report DESY 99-102.
7. see e.g. P.D.B. Collins, Introduction the Regge Theory and High Energy Physics, Cambridge University Press (1977).
8. J.J. Sakurai, Ann. Phys. 11 (1960) 1;
   J.J. Sakurai, Phys. Rev. Lett. 22 (1969) 981;
   H. Fraas and D. Schildknecht, Nucl. Phys. B14 (1969) 543.
9. D. Schildknecht, G.A. Schuler and B. Surrow, Phys. Lett. B449 (1999) 328.
10. A. Donnachie and P.V. Landshoff, Phys. Lett. B296 (1992) 227.
11. ZEUS Collab., M. Derrick et al., Phys. Lett. B350 (1995) 120;
    H1 Collab., S. Aid et al., Nucl. Phys., B472 (1996) 3;
    ZEUS Collab., J. Breitweg et al., Z. Phys. C75 (1997) 215.
12. M.G. Ryskin, Z. Phys. C57 (1993) 89;
    M.G. Ryskin et al., Z. Phys. C76 (1997) 231.
13. S. Brodsky et al., Phys. Rev. D50 (1994) 3134.
14. J. Nemchik, N.N. Nikolaev and B.G. Zakharov, Phys. Lett. B341 (1994) 228.
15. A. Donnachie and P.V. Landshoff, Phys. Lett. B348 (1995) 213.
16. L. Frankfurt, W. Koepf and M. Strikman, Phys. Rev. D54 (1996) 3194.
17. A.D. Martin, M.G. Ryskin and T. Teubner, Phys. Rev. D55 (1997) 4329.

18. J.R. Cudell and I. Royen, hep-ph/9807294.
19. D.Yu. Ivanov and R. Kirschner, Phys. Rev. D58 (1998) 114025.
20. E.V. Kuraev, N.N. Nikolaev and B.G. Zakharov, JETP Lett. 68 (1998) 696 and Pisma Zh. Eksp. Teor. Fiz. 68 (1998) 667;
N.N. Nikolaev, Proceedings of the DIS99 workshop, April 19-23, 1999, Zeuthen, Germany, Eds. J. Blumlein and T. Riemann, to apper in Nucl. Phys. B (Proc. Suppl.).
21. I. Royen, Proceedings of the DIS99 workshop, April 19-23, 1999, Zeuthen, Germany, Eds. J. Blumlein and T. Riemann, to apper in Nucl. Phys. B (Proc. Suppl.) and Liege University preprint ULC-PNT-99-1-IR.